

Admittance-Based Modeling of Cables and Overhead Lines by Idempotent Decomposition

Felipe Camara, Antonio C. S. Lima, Maria Teresa Correia de Barros, Filipe Faria da Silva, and Claus L. Bak

Abstract—This paper presents a new modeling approach based on idempotent decomposition of the nodal admittance matrix for representation of cables and overhead lines (OHL). By subjecting the idempotent matrices rather than the nodal admittance matrix to rational fitting, the poor observability of the smallest eigenvalues in the lower frequency range is overcome. Unlike the well-known method of characteristics (MoC), this alternative representation yields a so general fully-coupled admittance matrix suitable to tackle scenarios encompassing short and long lengths. Besides retaining the frequency dependence of parameters, the proposed phase-domain model showed to be accurate and suitable to circumvent the requirement of small time-steps.

Keywords—Cable, electromagnetic transients, idempotent decomposition, modeling, overhead line, vector fitting.

I. INTRODUCTION

THE field of cable modeling is an important research topic regarding simulation of electromagnetic transients (EMT). As a key enabler for integration of renewable energy resources, cables and overhead lines, hereinafter referred as lines, play an important role which requires accurate and efficient numerical models.

Time-domain solvers employ MoC-based models to evaluate traveling wave phenomena and several contributions have been proposed to overcome issues in modal-domain [1]–[11] and phase-coordinates [12]–[16]. Numerical stability is reported as a concern since large residue-pole ratios cause magnifications of interpolation errors leading to unstable time-domain simulations [17]–[20]. The influence of earth-return effects has receiving significant contributions since most parameter routines embedded in EMT-like software are based on conservative simplifying assumptions.

Simulations involving short line lengths require very small time-steps which increase the computation burden substantially. Some efforts addressed this problem [21], [22] but it has been traditionally coped by cascading π -sections

which precludes frequency dependent effects. To circumvent inherent issues related to MoC-based modeling, an alternative formulation exploits the nodal admittance matrix \mathbf{Y}_n [23], [24] which relates the terminal voltage and current in the frequency domain. It imposes no constraint due to the cable length, phase conductor arrangement or circuits running in parallel. However, the direct fitting of \mathbf{Y}_n results in inaccurate characterization of the smallest eigenvalues in the lower frequency range. The so-called *folded line equivalent* model [25] addressed this issue through a similarity transformation in \mathbf{Y}_n by decomposing it into open-circuit and short-circuit contributions in the phase-domain. Another distinct approach called Bergeron-cells [26] has been proposed for frequency-dependent modeling of transmission lines employing a cascade of cells in a similar fashion as in the cascaded π modeling. This methodology avoids the modal decomposition either in the identification and time-domain realization stages.

Commonly used in linear algebra, also known as spectral decomposition, the idempotent decomposition is a technique to decompose a given matrix into a sum of elementary matrices that, when multiplied by itself, produces itself again [27]. To the best of the author's knowledge, the first use of idempotents in power systems is reported to Prof. Wedepohl's lecture notes [28]. Then, the idempotent decomposition was firstly proposed in the rational approximation of \mathbf{H} in phase-coordinates for overhead lines [29]. Contrary to the modal domain transformation, it represents a linear transformation on idempotents instead of eigenvectors [30], [31]. Later, the feasibility of applying idempotents for a full-frequency dependent line model using the MoC was investigated in the analysis of underground cables and overhead lines [32]. However, it was found that the accuracy is dependent on the number of circuits running in parallel due to coupling effects. In a similar way, this paper investigates the concept of idempotents as a similarity transformation for decomposition of \mathbf{Y}_n into the sum of products of idempotent matrices to overcome numerical issues related to low observability of eigenvalues for phase-coordinates modeling. Due to the fully-coupled structure of the admittance matrix, it is foreseen the applicability of this approach to represent cables and overhead lines in real-time or multi-scale simulations [33] to tackle short and long lengths.

This paper is organised as follows: Section 2 presents the available formulations to derive a wideband model for EMT computations. Section 3 presents the idempotent decomposition and how it can be implemented to allow the interface with time-domain solvers. In Section 4, the proposed

This work was supported in part by the European Union's Horizon 2020 research and innovation programme under the Marie Skłodowska-Curie grant agreement No 101031088, Coordenação de Aperfeiçoamento de Pessoal de Nível Superior (CAPES) under Grant 001, Conselho Nacional de Desenvolvimento Científico e Tecnológico (CNPq) under grants 404068/2020-0, 400851/2021-0, Fundação de Amparo à Pesquisa do Estado de Minas Gerais (FAPEMIG) under grant APQ-03609-17 and Instituto Nacional de Energia Elétrica (INERGE).

F. Camara, F.M.F. Silva and C.L. Bak are with Aalborg University, Denmark, (emails: fcn@energy.aau.dk, ffs@et.aau.dk, clb@et.aau.dk). A.C.S. Lima is with the Federal University of Rio de Janeiro, Brazil, (email: acsl@dee.ufrj.br). M.T. Correia de Barros is with University of Lisbon, Portugal, (email: teresa.correiaedebarras@tecnico.ulisboa.pt).

Paper submitted to the International Conference on Power Systems Transients (IPST2023) in Thessaloniki, Greece, June 12-15, 2023.

formulation is validated through comparison with standard time-domain simulations. Finally, Section 5 presents the main conclusions.

II. TIME-DOMAIN MODELING

A. Method of Characteristics (MoC)

Time-domain solvers resort to MoC models to represent cables in transient studies. Also known as traveling-wave method, it is based on propagation parameters given by the characteristic admittance \mathbf{Y}_c and the propagation function \mathbf{H} . It consists the full representation of the distributed nature of transmission line impedances together with the skin effect and earth-return path influence. The formulation in the frequency-domain is given as follows [34]

$$\mathbf{I}_k = \mathbf{Y}_c \mathbf{V}_k - \mathbf{H} [\mathbf{Y}_c \mathbf{V}_m + \mathbf{I}_m] \quad (1a)$$

$$\mathbf{I}_m = \mathbf{Y}_c \mathbf{V}_m - \mathbf{H} [\mathbf{Y}_c \mathbf{V}_k + \mathbf{I}_k] \quad (1b)$$

where \mathbf{Y}_c is the characteristic admittance and \mathbf{H} is the propagation function given by

$$\begin{aligned} \mathbf{Y}_c &= \mathbf{Z}^{-1} \sqrt{\mathbf{Z}\mathbf{Y}} \\ \mathbf{H} &= \exp\left(-\ell \sqrt{\mathbf{Y}\mathbf{Z}}\right) \end{aligned} \quad (2)$$

in which \mathbf{Z} and \mathbf{Y} are the series impedance and shunt admittance matrices per unit length and ℓ is the line length. The time-domain counterparts obtained by means of convolutions are given by

$$\mathbf{i}_k = \mathbf{y}_c * \mathbf{v}_k - \mathbf{h} * [\mathbf{y}_c * \mathbf{v}_m + \mathbf{i}_m] \quad (3a)$$

$$\mathbf{i}_m = \mathbf{y}_c * \mathbf{v}_m - \mathbf{h} * [\mathbf{y}_c * \mathbf{v}_k + \mathbf{i}_k] \quad (3b)$$

as \mathbf{y}_c and \mathbf{h} are the unit impulse responses of \mathbf{Y}_c and \mathbf{H} , \mathbf{v}_k , \mathbf{v}_m , \mathbf{i}_k and \mathbf{i}_m are the terminal voltages and injected currents and the symbol $*$ indicates convolution. The implementation of MoC-based models requires \mathbf{Y}_c and \mathbf{H} matrices to be subjected to a rational approximation. Even though the resulting approximation correspond to a passive rational model within a user-defined band, numerical issues still might occur [17], [18], [35].

B. Nodal Admittance Matrix

The modeling through the nodal admittance matrix \mathbf{Y}_n in the frequency domain provides a more compact form without the requirement to handle \mathbf{Y}_c and \mathbf{H} matrices in an explicitly way. After subjected to a rational approximation, \mathbf{Y}_n presents the following form

$$\mathbf{Y}_n(s) \approx \sum_{m=1}^M \frac{\mathbf{R}_m}{s - p_m} + \mathbf{D} \quad (4)$$

where p_m is a set of common poles, either real or complex conjugate, \mathbf{R}_m is the residue matrix and \mathbf{D} is the real part of \mathbf{Y}_n at infinite frequency.

Let a cable consisting of n phases or metallic conductors, \mathbf{Y}_n is given by

$$\mathbf{Y}_n(s) = \begin{bmatrix} \mathbf{Y}_s & \mathbf{Y}_m \\ \mathbf{Y}_m & \mathbf{Y}_s \end{bmatrix} \quad (5)$$

where \mathbf{Y}_s and \mathbf{Y}_m are $n \times n$ block matrices defined by

$$\mathbf{Y}_s = \mathbf{Y}_c (\mathbf{I} + \mathbf{H}^2) (\mathbf{I} - \mathbf{H}^2)^{-1} \quad (6a)$$

$$\mathbf{Y}_m = -2 \mathbf{Y}_c \mathbf{H} (\mathbf{I} - \mathbf{H}^2)^{-1} \quad (6b)$$

and \mathbf{I} is an $n \times n$ identity matrix. The direct fitting of \mathbf{Y}_n often results in inaccurate characterization of small eigenvalues at low frequencies as a consequence of a large eigenvalue ratio. This common issue can be overcome resorting to the the *Modal Vector Fitting* (MVF) [36], even though the computation time can be substantial, or to the *Mode-Revealing Transformation* (MRT) [37] or *Folded Line Equivalent* [25] schemes.

III. IDEMPOTENT DECOMPOSITION

As aforementioned, the idempotent decomposition represents a linear transformation. In [32], the identification of \mathbf{H} matrix was carried out by means of a sum of products of idempotent matrices as an alternative to the modal grouping in the original proposition of the so-called Universal Line Model (ULM) [12]. Here, an eigendecomposition of \mathbf{Y}_n is performed instead, resulting in the so-called idempotent matrices. These matrices are accomplished by the product of a frequency dependent transformation matrix \mathbf{T} , a diagonal matrix of modes \mathbf{Y}_m and the inverse matrix of \mathbf{T} given by

$$\mathbf{Y}_n(s) = \mathbf{T} \cdot \mathbf{Y}_m \cdot \mathbf{T}^{-1} \quad (7)$$

Writing the transformation matrices \mathbf{T} and \mathbf{T}^{-1} in terms of their respective rows \mathbf{r}_i and columns \mathbf{c}_i

$$\begin{aligned} \mathbf{Y}_n(s) &= [\mathbf{c}_1 \quad \dots \quad \mathbf{c}_n] \begin{bmatrix} y_1 & & \\ & \ddots & \\ & & y_n \end{bmatrix} \begin{bmatrix} \mathbf{r}_1 \\ \vdots \\ \mathbf{r}_n \end{bmatrix} \\ \mathbf{Y}_n(s) &= [\mathbf{c}_1 \mathbf{r}_1] y_1 + \dots + [\mathbf{c}_n \mathbf{r}_n] y_n \\ \mathbf{Y}_n(s) &= \sum_{i=1}^n \mathbf{M}_i y_i \end{aligned} \quad (8)$$

where n is the number of modes and \mathbf{M}_i are the idempotent matrices to be subjected to rational approximation with the *Vector Fitting* routine [38]–[41].

Aiming at lowering the order of the rational functions, the proposition to group idempotent matrices will be employed in a similar fashion like the grouping routine used in the ULM approach. Then, the grouping scheme sums up the idempotent matrices that have eigenvalues exhibiting similar behavior, as sketched in (9).

$$\mathbf{Y}_n(s) = \mathbf{M}_1 + \mathbf{M}_2 = \sum_{i=1}^{n_1} \mathbf{M}_i y_i + \sum_{i=n_1+1}^n \mathbf{M}_i y_i \quad (9)$$

where n_1 is the number of modes considered for deriving \mathbf{M}_1 and the remaining ones are considered for deriving \mathbf{M}_2 . It is worth mentioning that the time delay extraction is disregarded since \mathbf{Y}_n inherits the propagation delays through its block matrices derived from \mathbf{H} . Thus, it is implicitly considered in the \mathbf{M}_i matrices.

For time-domain implementation of the proposed idempotent model, the procedure is slightly different

from the implementation based on the direct fitting of the nodal admittance matrix \mathbf{Y}_n . Since \mathbf{Y}_n was decomposed into a sum of independent matrices, the equivalent history current source should be represented as a set of parallel current sources associated with each idempotent matrix \mathbf{M}_i , as depicted in Fig. 1. Assuming the grouping scheme yields two idempotent matrices, one has to update two current sources separately. Thus, the equivalent source is obtained by summing both contributions.

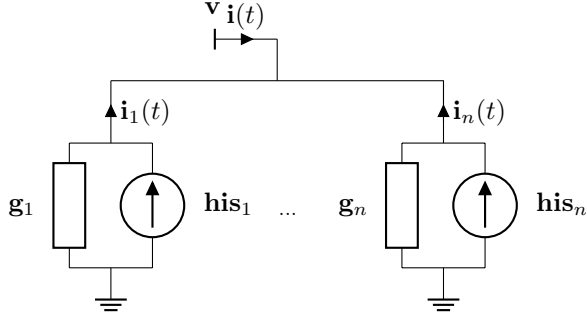


Fig. 1. Time-domain realization of a idempotent line model

A brief discription on the expressions to calculate the history current source for each idempotent group is provided in Appendix A.

IV. TEST CASES

The accuracy of the proposed idempotent model is demonstrated with three test cases, namely:

- 1) case #1: single-core HVDC submarine cable, 2.5 km
- 2) case #2: 132-kV overhead line, 10 km

A frequency-domain algorithm based on the Numerical Laplace Transform (NLT) [42]–[44] is employed for the sake of validation. Once the whole network is solved in the complex frequency domain, it can be considered as an accurate response. The abovementioned user-defined codes and the one to obtain the nodal admittance matrix were developed with

A. Case #1: HVDC Cable

Let a single core (SC) armoured submarine cable employed in a VSC–HVDC link [45]. In such applications, the cables are buried just below the seabed, with depths varying from 1 to 2 m. Here, the burial depth is 1.5 m below the seabed and the cable is 2.5 km long. The cross-section is depicted in Fig. 2 and the reader is referred to Appendix B to assess the main data.

Firstly, the cable parameters were computed in the frequency range between 0.01 Hz – 1 MHz to extract the nodal admittance matrix \mathbf{Y}_n as stated in (5). It was considered a combination of linearly and logarithmically spaced frequency samples. Linear sampling provides a good resolution at low frequencies, while logarithmic sampling provides better resolution at high frequencies and when the frequency response of a given system exhibits significant changes in amplitude. When \mathbf{Y}_n is subjected to a direct fitting, a poor observation of the eigenvalues at low frequencies is

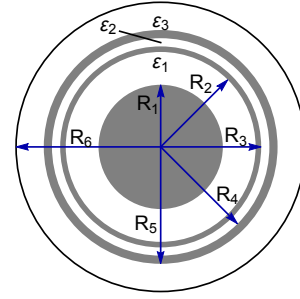


Fig. 2. Case #1: 75 kV HVDC submarine cable configuration

observed even with a passived rational approximation of the original matrix \mathbf{Y}_n , as shown in Fig. 3 and Fig. 4.

The proposed methodology consists in decomposing \mathbf{Y}_n into idempotent matrices and then applying the grouping scheme of modes with close eigenvalues. Naturally, each $\mathbf{M}_i \mathbf{y}_i$ could be fitted independently, as described in (8), although this would lead to a considerably larger model. It can be observed in Fig. 4 two mode groups with distinct behaviour at the lower frequency range. Thus, we can group their respective idempotent counterparts to lower the amount of matrices to be subjected to rational approximation with the VF routine.

In this example, the eigendecomposition of \mathbf{Y}_n yields six eigenvalues or modes and it was possible to reduce the six idempotent matrices into two equivalent groups, namely, \mathbf{M}_1 and \mathbf{M}_2 . Fig. 5 shows the elements of each matrix and the resulting pole-residue model with 70 and 90 poles, respectively, is presented in Fig. 6.

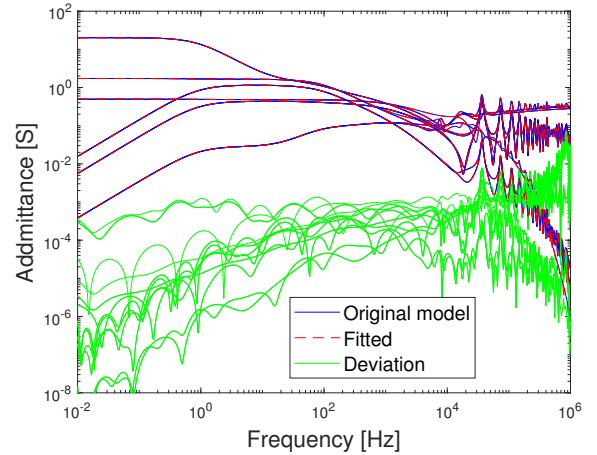


Fig. 3. Case #1: Rational fitting of \mathbf{Y}_n

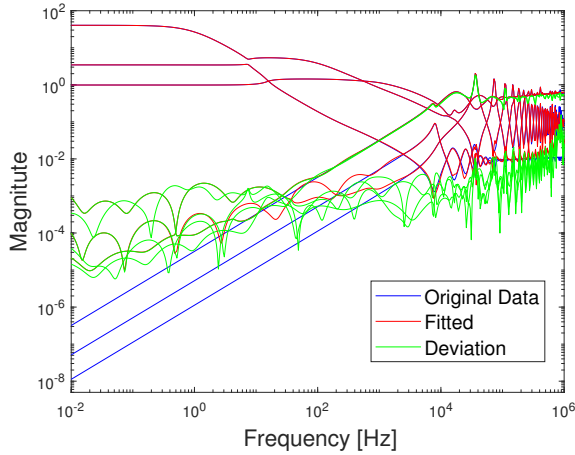


Fig. 4. Case #1: Eigenvalues of \mathbf{Y}_n

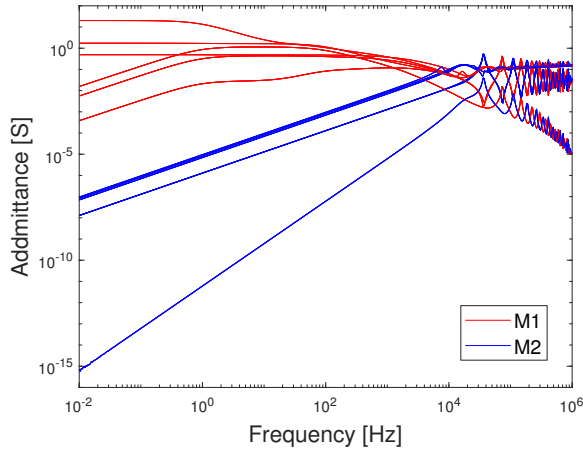
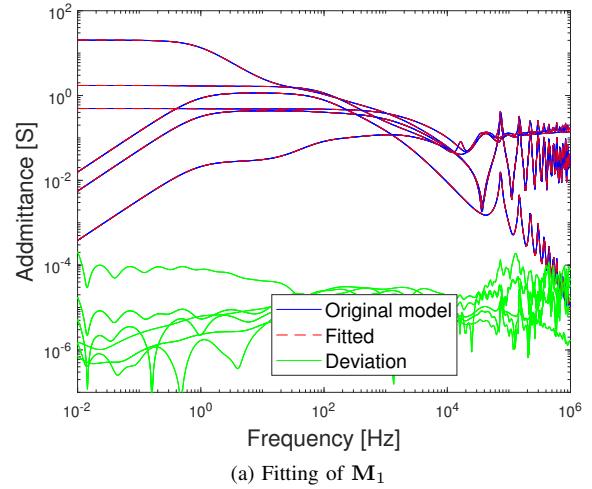
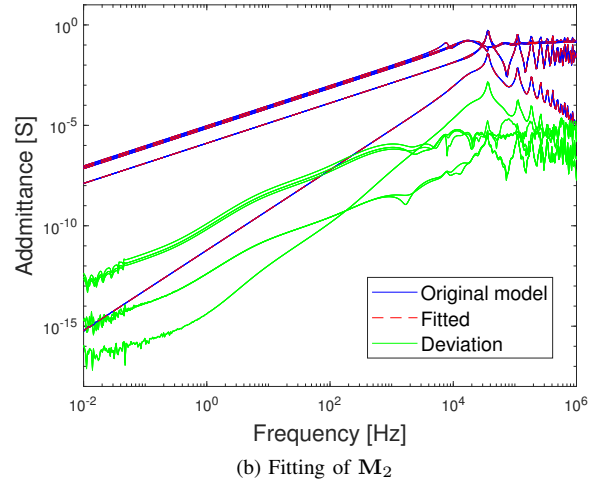


Fig. 5. Case #1: Idempotent matrices

To evaluate the accuracy of the proposed idempotent model in the time-domain with the NLT algorithm, a voltage source is ramped up linearly to 1 V in $50 \mu\text{s}$ at the core conductor as depicted in Fig. 7. To obtain a more oscillatory waveform, the sheath and armour conductors are bolted together and left ungrounded at both terminals. A time-step of $\Delta t = 5 \mu\text{s}$ is assumed. The simulated core and sheath voltages at the receiving end are shown in Fig. 8 and the validation is done with the results obtained with the NLT algorithm. In a similar fashion, the current in the core conductor is shown in Fig. 9 and again a very accurate match is attained.



(a) Fitting of \mathbf{M}_1



(b) Fitting of \mathbf{M}_2

Fig. 6. Case #1: Fitting results (HVDC submarine cable)

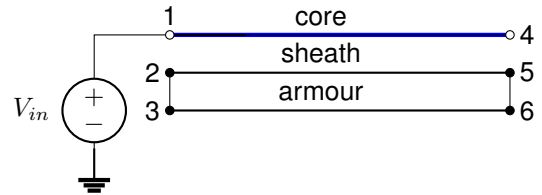


Fig. 7. Case #1: Circuit for time-domain simulation

B. Case #2: Overhead Line

The versatility of the idempotent model is to be verified by assessing the modeling of an overhead line (OHL). The simulation comprises a 10 km untransposed line while the ground wires are assumed continuously grounded [46], as shown in Fig. 10.

For this configuration, which presents a natural resonance frequency around 7.5 kHz, a combination of linearly and logarithmically spaced samples in the frequency range between 0.01 Hz – 150 kHz was considered to extract the nodal admittance matrix \mathbf{Y}_n . The idempotent decomposition was then performed and the grouping scheme resulted in two idempotent matrices \mathbf{M}_1 and \mathbf{M}_2 . The resulting rational

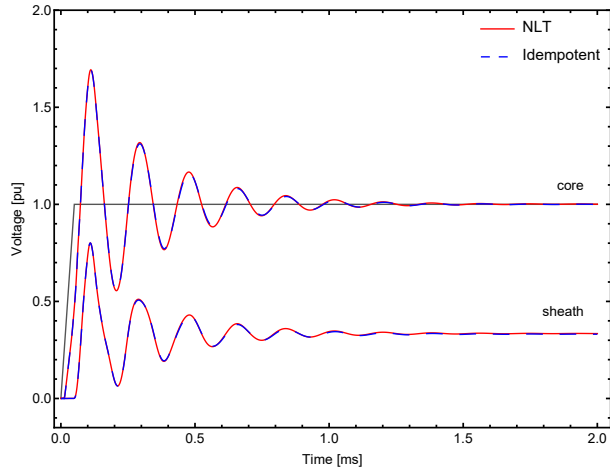


Fig. 8. Case #1: Receiving end voltage

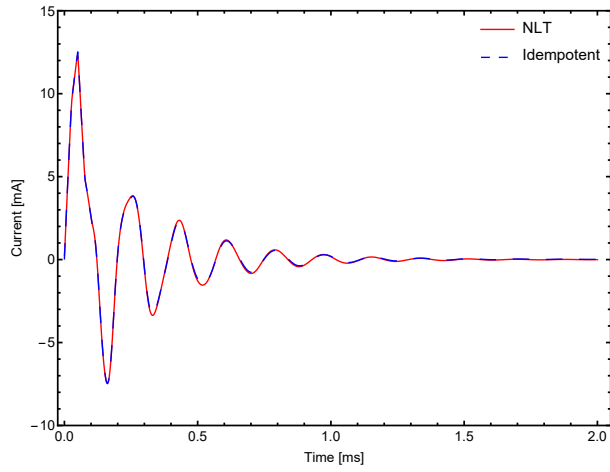


Fig. 9. Case #1: Current at terminal #1

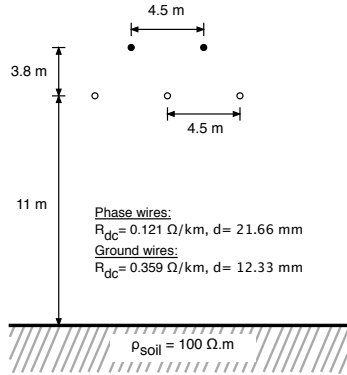
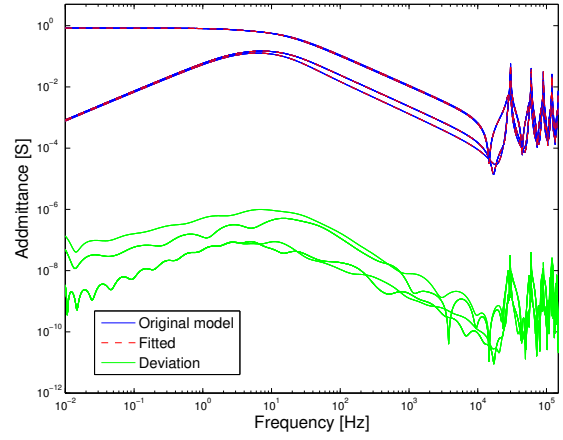


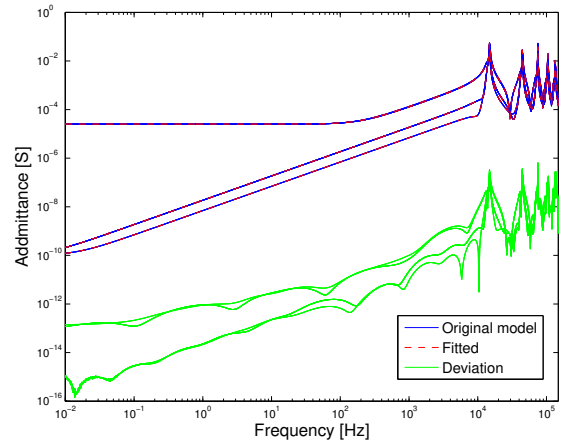
Fig. 10. Case #2: 132-kV transmission line geometry

models were achieved with 60 and 50 poles for M_1 and M_2 , respectively, as shown in Fig. 11.

Fig. 12 shows the case representing a single-phase energization where the OHL receiving end is open-circuited. It is assumed a short-circuit reactance behind the voltage source. The simulated voltage at terminal #4 is presented in Fig. 13 and the current at terminal #1 is presented in Fig. 14. Employing a time-step of $\Delta t = 10 \mu s$, a very accurate match



(a) Fitting of M_1



(b) Fitting of M_2

Fig. 11. Case #2: Fitting results

is observed without substantial loss of accuracy in comparison with the NLT algorithm.

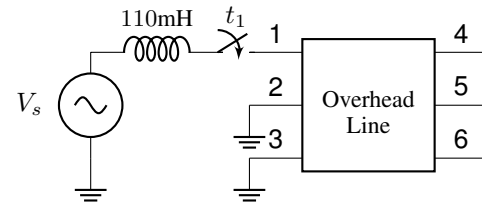


Fig. 12. Case #1: Circuit for time-domain simulation

V. CONCLUSIONS

This paper has introduced a new approach for simulation of electromagnetic transients involving cables and overhead lines in phase-coordinates exploiting the fully-coupled structure of the admittance matrix. Resorting to the idempotent decomposition, it showed to be a feasible alternative to circumvent the poor rational fitting of the smallest eigenvalues of the nodal admittance matrix Y_n at the lower

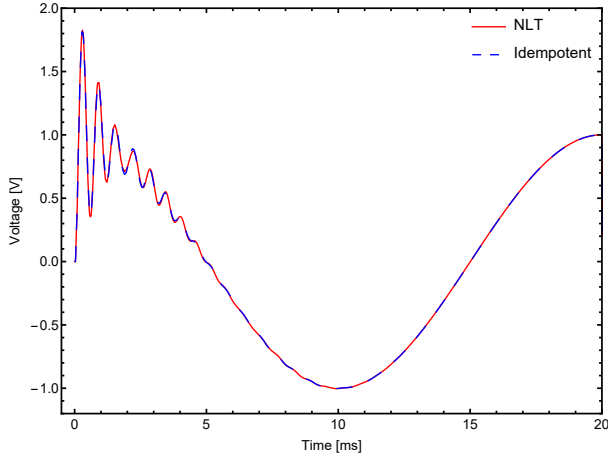


Fig. 13. Case #2: Receiving end voltage at terminal # 4

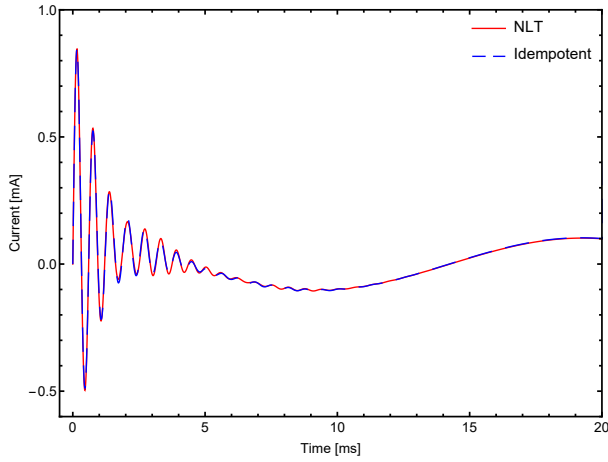


Fig. 14. Case #2: Current at terminal # 1

frequency range providing accurate time-domain results. The idempotent model is particularly useful as an alternative to the well-known MoC-based model to handle time-step constraints associated with traveling-wave times in the presence of short and long cable lengths when simulating bulky power systems. Furthermore, has the benefit of handling highly coupled arrangements like parallel circuits. It allows to avoid the replacement of short line lengths by a frequency independent equivalent π -circuit inasmuch as the frequency dependence can be taken into account.

APPENDIX

A. State-space realization

Consider a scalar element with the following transfer function in the frequency domain

$$I(s) = \frac{r}{s-a} V(s) + dV(s) \quad (10)$$

where $V(s)$ and $I(s)$ are the complex voltage and current, r , d and a are real. In the time-domain, it is possible to rewrite (10) as

$$\begin{aligned} \dot{x}(t) &= ax(t) + bv(t) \\ i(t) &= rx(t) + dv(t) \end{aligned} \quad (11)$$

Using either the trapezoidal rule of integration or recursive convolution leads to the following discrete time equivalent

$$\begin{aligned} x(n) &= \alpha x(n-1) + (\alpha\lambda + \mu) v(n-1) \\ i(n) &= x(n) + (\lambda + d) v(n) \end{aligned} \quad (12)$$

where the coefficients α , λ and μ are given by (13) if trapezoidal rule is applied

$$\alpha = \frac{2 + a\Delta t}{2 - a\Delta t} \quad \lambda = \mu = \frac{r\Delta t}{2 - a\Delta t} \quad (13)$$

and in the case recursive convolutions are considered

$$\begin{aligned} \alpha &= \exp(a\Delta t) & \lambda &= -\frac{r}{a} \left(1 + \frac{1-\alpha}{a\Delta t}\right) \\ \mu &= \frac{r}{a} \left(\alpha + \frac{1-\alpha}{a\Delta t}\right) \end{aligned} \quad (14)$$

The equation in (12) represents a companion network where

$$i(n) = his(n) + gv(n) \quad (15)$$

with

$$\begin{aligned} his(n) &= \alpha his(n-1) + cv(n-1) \\ g &= \lambda + d \\ c &= \alpha\lambda + \mu \end{aligned} \quad (16)$$

B. HVDC Cable data

TABLE I
CASE #1: SUBMARINE CABLE DATA

Core conductor	$R_1 = 18.95$ mm	$\rho_c = 1.723 \times 10^{-8}$ Ω .m
First insulation layer	$R_2 = 28.95$ mm	$\varepsilon_1 = 2.5$
Sheath	$R_3 = 30.65$ mm	$\rho_s = 22 \times 10^{-8}$ Ω .m
Second insulation layer	$R_4 = 33.15$ mm	$\varepsilon_2 = 2.5$
Armour	$R_5 = 35.65$ mm	$\rho_a = 11 \times 10^{-8}$ Ω .m, $\mu_a = 90$
Armour insulation	$R_6 = 44.10$ mm	$\varepsilon_3 = 2.5$

REFERENCES

- [1] H. Nakanishi and A. Ametani, "Transient calculation of a transmission line using superposition law," *IEE Proceedings C - Generation, Transmission and Distribution*, vol. 133, no. 5, pp. 263–269, July 1986.
- [2] G. Angelidis and A. Semlyen, "Direct phase-domain calculation of transmission line transients using two-sided recursions," *IEEE Trans. on Power Delivery*, vol. 10, no. 2, pp. 941–949, April 1995.
- [3] B. Gustavsen, J. Sletbak, and T. Henriksen, "Calculation of the electromagnetic transients in transmission cables and lines taking frequency dependent effects accurately account," *IEEE Trans. on Power Delivery*, vol. 10, no. 2, pp. 1076–1084, April 1995.
- [4] T. Noda, N. Nagaoka, and A. Ametani, "Phase-domain modeling of frequency-dependent transmission lines by means of an arma model," *IEEE Transactions on Power Delivery*, vol. 11, no. 1, pp. 401–411, Jan 1996.
- [5] H. Nguyen, H. Dommel, and J. Marti, "Direct phase-domain modelling of frequency-dependent overhead transmission lines," *IEEE Transactions on Power Delivery*, vol. 12, no. 3, pp. 916–921, July 1997.
- [6] B. Gustavsen and A. Semlyen, "Calculation of transmission line transients using polar decomposition," *IEEE Transactions on Power Delivery*, vol. 13, no. 3, pp. 855–862, July 1998.
- [7] —, "Combined phase and modal domain calculation of transmission line transients based on vector fitting," *IEEE Transactions on Power Delivery*, vol. 13, no. 2, pp. 596–604, April 1998.
- [8] T. C. Yu and J. Marti, "A robust phase-coordinates frequency-dependent underground cable model (zcable) for the emtp," *IEEE Transactions on Power Delivery*, vol. 18, no. 1, pp. 189–194, January 2003.

- [9] A. B. Fernandes and W. L. A. Neves, "Phase-domain transmission line models considering frequency-dependent transformation matrices," *IEEE Transactions on Power Delivery*, vol. 19, no. 2, pp. 708–714, April 2004.
- [10] T. Noda, "Application of frequency-partitioning fitting to the phase-domain frequency-dependent modeling of overhead transmission lines," *IEEE Transactions on Power Delivery*, vol. 30, no. 01, pp. 174–183, February 2015.
- [11] —, "Application of frequency-partitioning fitting to the phase-domain frequency-dependent modeling of underground cables," *IEEE Transactions on Power Delivery*, vol. 31, no. 4, pp. 1776–1777, August 2016.
- [12] A. Morched, B. Gustavsen, and M. Tartibi, "A universal model for accurate calculation of electromagnetic transients on overhead lines and underground cables," *IEEE Transactions on Power Delivery*, vol. 14, no. 3, pp. 1032–1038, July 1999.
- [13] H. D. Silva, A. Gole, and L. Wedepohl, "Accurate electromagnetic transient simulations of hvdc cables and overhead transmission lines," *International Conference on Power System Transients (IPST)*, June 2007.
- [14] B. Gustavsen and J. Nordstrom, "Pole identification for the universal line model based on trace fitting," *IEEE Transactions on Power Delivery*, vol. 23, no. 1, pp. 472–479, January 2008.
- [15] A. Ramirez and R. Irvani, "Enhanced fitting to obtain an accurate dc response of transmission lines in the analysis of electromagnetic transients," *IEEE Transactions on Power Delivery*, vol. 29, no. 6, pp. 2614 – 2621, 2014.
- [16] I. Kocar and J. Mahseredjian, "New procedure for computation of time delays in propagation function fitting for transient modeling of cables," *IEEE Transactions on Power Delivery*, vol. 31, no. 2, pp. 613–621, 2016.
- [17] I. Kocar, J. Mahseredjian, and G. Olivier, "Improvement of numerical stability for the computation of transients in lines and cables," *IEEE Transactions on Power Delivery*, vol. 25, no. 2, pp. 1104–1111, April 2010.
- [18] B. Gustavsen, "Avoiding numerical instabilities in the universal line model by a two-segment interpolation scheme," *IEEE Transactions on Power Delivery*, vol. 28, no. 3, pp. 1643–1651, July 2013.
- [19] I. Kocar and J. Mahseredjian, "Accurate frequency dependent cable model for electromagnetic transients," *IEEE Transactions on Power Delivery*, vol. 31, no. 3, pp. 1281 – 1288, 2016.
- [20] M. Cervantes, I. Kocar, J. Mahseredjian, and A. Ramirez, "Partitioned fitting and dc correction for the simulation of electromagnetic transients in transmission lines/cables," *IEEE Transactions on Power Delivery*, vol. 33, no. 6, pp. 3246–3248, 2018.
- [21] S. Henschel, A. Ibrahim, and H. Dommel, "Transmission line model for variable step size simulation algorithms," *International Journal on Electric Power and Energy Systems*, vol. 21, no. 03, pp. 191–198, March 1999.
- [22] A. Ibrahima, S. Henschelb, A. C. S. Lima, and H. Dommel, "Applications of a new emtp line model for short overhead lines and cables," *International Journal on Electric Power and Energy Systems*, vol. 24, no. 08, pp. 639–645, October 2002.
- [23] N. Nagaoka and A. Ametani, "Transient calculations on crossbonded cables," *IEEE Transactions on Power Apparatus and Systems*, vol. PAS-102, no. 4, pp. 779–787, 1983.
- [24] I. Lafaia, J. Mahseredjian, A. Ametani, M. T. Correia de Barros, I. Koçar, and Y. Fillion, "Frequency and time domain responses of cross-bonded cables," *IEEE Transactions on Power Delivery*, vol. 33, no. 2, pp. 640–648, 2018.
- [25] B. Gustavsen and A. Semlyen, "Admittance-based modeling of transmission lines by a folded line equivalent," *IEEE Transactions on Power Delivery*, vol. 24, no. 1, pp. 231–239, January 2009.
- [26] T. Noda, "Frequency-dependent modeling of transmission lines using bergeron cells," *IEEE Transactions on Electrical and Electronic Engineering*, vol. 12, no. S2, pp. S23–S30, 2017. [Online]. Available: <https://onlinelibrary.wiley.com/doi/abs/10.1002/tee.22564>
- [27] G. Strang, *Linear Algebra and Its Applications*. Cengage Learning, 2006.
- [28] L. M. Wedepohl, *Frequency Domain Analysis of Wave Propagation in Multiconductor Transmission Systems (Lecture notes)*, The University of British Columbia, Dept. of Electrical Engineering, Vancouver, Canada, 1993.
- [29] F. Castellanos and J. Marti, "Phase-domain multiphase transmission line models," *International Conference on Power System Transients (IPST)*, pp. 17–22, September 1995.
- [30] F. Castellanos, J. Marti, and F. Marcano, "Phase-domain multiphase transmission line models," *Electrical Power & Energy Systems*, vol. 19, no. 4, pp. 241–248, 1997, elsevier Science Ltd.
- [31] F. Marcano and J. Marti, "Idempotent line model: Case studies," in *Proceedings of IPST'97 - International Conference on Power Systems Transients*, 1997, pp. 67–72.
- [32] M. Y. Tomasevich and A. C. Lima, "Some developments on phase coordinates line modeling based on idempotent decomposition," *International Journal of Electrical Power & Energy Systems*, vol. 74, pp. 410–419, 2016.
- [33] F. Camara, A. C. Lima, and K. Strunz, "Multi-scale formulation of admittance-based modeling of cables," *Electric Power Systems Research*, vol. 195, pp. 107–120, 2021.
- [34] J. A. Martinez, Ed., *Power System Transients: Parameter Determination*. CRC Press, 2010.
- [35] B. Gustavsen, "Passivity enforcement for transmission line models based on the method of characteristics," *IEEE Transactions on Power Delivery*, vol. 24, no. 3, pp. 2286–2293, October 2008.
- [36] B. Gustavsen and C. Heitz, "Modal vector fitting: A tool for generating rational models of high accuracy with arbitrary terminal conditions," *IEEE Transactions on Advanced Packaging*, vol. 31, no. 4, pp. 664–672, November 2008.
- [37] B. Gustavsen, "Rational modeling of multiport systems via a symmetry and passivity preserving mode-revealing transformation," *IEEE Transactions on Power Delivery*, vol. 29, no. 1, pp. 199–206, February 2014.
- [38] B. Gustavsen and A. Semlyen, "Rational approximation of frequency domain responses by vector fitting," *IEEE Transactions on Power Delivery*, vol. 14, no. 3, pp. 1052–1061, July 1999.
- [39] B. Gustavsen, "Rational approximation of frequency dependent admittance matrices," *IEEE Transactions on Power Delivery*, vol. 17, no. 4, pp. 1093–1098, 2002.
- [40] —, "Improving the pole relocating properties of vector fitting," *IEEE Transactions on Power Delivery*, vol. 21, no. 03, pp. 1587–1592, July 2006.
- [41] D. Deschrijver, M. Mrozowski, T. Dhaene, and D. D. Zutter, "Macromodeling of multiport systems using a fast implementation of the vector fitting method," *IEEE Microwave and Wireless Components Letters*, vol. 18, no. 6, pp. 383–385, June 2008.
- [42] D. J. Wilcox, "Numerical Laplace Transformation and Inversion," *International Journal Elect. Eng.*, vol. 15, pp. 247–265, 1978.
- [43] F. A. Uribe, J. L. Naredo, and P. Moreno, "Electromagnetic transients in underground transmission systems through the numerical laplace transform," *International Journal of Electrical Power & Energy Systems*, vol. 24, no. 3, pp. 215–221, March 2002.
- [44] P. Moreno and A. Ramirez, "Implementation of the numerical laplace transform: A review (task force on frequency domain methods for emt studies)," *IEEE Transactions on Power Delivery*, vol. 23, no. 4, pp. 2599–2609, October 2008.
- [45] C. H. Chien and R. W. G. Bucknall, "Analysis of harmonics in subsea power transmission cables used in vsc-hvdc transmission systems operating under steady-state conditions," *IEEE Transactions on Power Delivery*, vol. 22, no. 4, pp. 2489–2497, October 2007.
- [46] B. Gustavsen, "Validation of frequency dependent transmission line models," *IEEE Transactions on Power Delivery*, vol. 2, no. 2, pp. 925–933, April 2005.